The influence of aluminum trichloride on a configuratively labile lactone-bridged biaryl: quantum chemical calculations and optical spectroscopy*

Gerhard Bringmann**, Ulrich Dauer and Olaf Schupp
Institut für Organische Chemie, Universität Würzburg, Am Hubland, D-97074 Würzburg (Germany)

Markus Lankers, Jürgen Popp, Uwe Posset, Andrea Weippert and Wolfgang Kiefer**
Institut für Physikalische Chemie, Universität Würzburg, Marcusstrasse 9-11, D-97070 Würzburg (Germany)

(Received January 10, 1994)

Abstract

Semiempirical and *ab initio* calculations on the binding properties of the $AlCl_3$ complex of 1,3-dimethylbenzo[*b*]naphtho[1,2-*d*]pyran-6-one are reported. Compounds of this type are key intermediates in the stereoselective synthesis of axially chiral biaryl systems. Semiempirical (MNDO, PM3) and *ab initio* (STO-3G, 3-21G) calculations give important information about conformational changes that occur by complexing the free lactone with $AlCl_3$: the calculations predict a significant influence on the lengths of the $(C{=}O)_{exo}$ and $(C{-}O)_{endo}$ bonds, and a distinct planarization of the heterocyclic lactone part of the complexed benzonaphthopyranone. IR and Raman spectroscopy was applied in order to confirm the theoretical predictions. The good agreement of results obtained by semiempirical frequency calculations with the experimental data supports the assignment of vibrational bands affected on coordination. The highest shift caused by coordination (-152 cm^{-1}) is observed for ν(C=O).

Key words: Quantum chemical calculations; Optical spectroscopy; Aluminum complexes; Lactone complexes; Benzonaphthopyranone

Introduction

Benzonaphthopyranones like **1** constitute synthetically valuable precursors to configuratively stable enantiomerically pure biaryl target molecules like **2**, into which they can be transformed by a novel atropisomer-selective ring opening reaction [2]. This stereochemically intriguing cleavage process, in the course of which the axially prostereogenic (i.e. configuratively labile) biaryl axis is 'twisted' to give a configuratively stable axis of any desired absolute configuration, can be brought about using various types of chiral H-, O- or N-nucleophiles [3–5]. Due to the modest carbonyl reactivity of the lactone functionality, these nucleophiles have hitherto been applied in a deprotonated, i.e. metal activated, form of the general type $NuML_n^{\neg}$* (Scheme 1) [6]. An alternative approach is based on a preceding activation of the carbonyl group by Lewis acids, and the resulting complex **3** should then readily react even with neutral, non-anionized chiral nucleophiles Nu*. A highly attractive future goal would finally be to use a chiral Lewis acid $ML_n^{\neg}$*, possibly even in only catalytic amounts, and subsequently perform the ring opening reaction with cheap, achiral and simple nucleophiles Nu (Scheme 1). As a first step in this direction, we have recently prepared and spectroscopically investigated first transition metal complexes of the general type **3** (e.g. M=Zr, Re) [7, 8].

Vibrational spectroscopy is a most potent tool for the investigation of structural details of such molecules, especially if paralleled by the computational prediction of structural and spectroscopic data using modern semiempirical or *ab initio* methods [9]. We have recently performed a normal coordinate analysis on a metal-free simplified analog of **1** (with the two methyl groups replaced by hydrogen atoms) [10]. In this paper, we report on the influence of Lewis acids on the binding properties of lactones of this type such as force constants and bond distances, exemplified by complex **4** resulting from the reaction of **1** and the simple main group Lewis

*Part 39 of the series 'Novel Concepts in Directed Biaryl Synthesis'; for Part 38 see ref. 1.

**Authors to whom correspondence should be addressed.

SSDI 0020-1693(94)03915-B

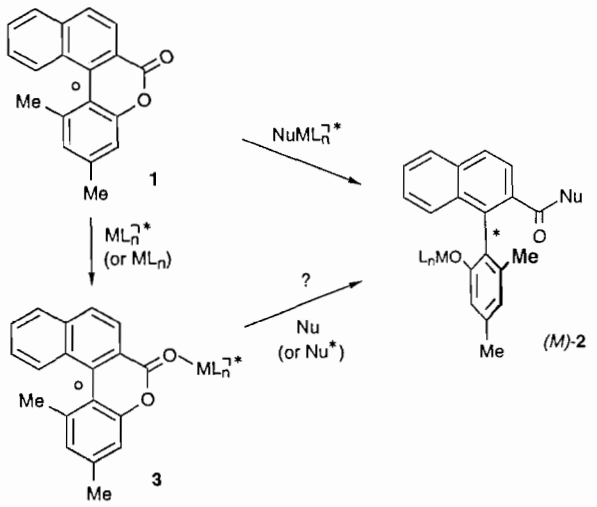

Scheme 1. A novel concept for the metal assisted atropisomer selective cleavage of biaryl lactones to chiral biaryl systems. Stable stereogenic elements (axes or centers) are denoted by *, unstable ones by ○.

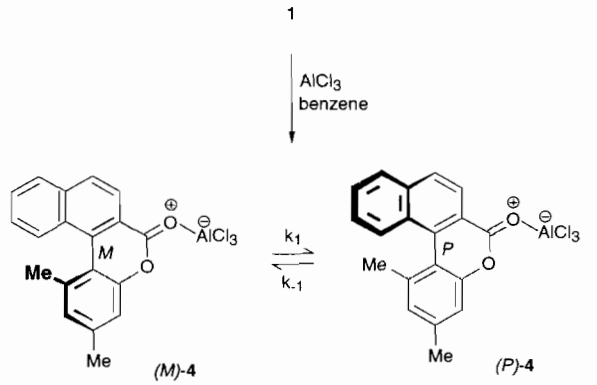

Scheme 2. Preparation and helimerization of the stereochemically labile complex **4**.

acid $AlCl_3$ (Scheme 2). The assignment of the vibrational modes, as influenced by the coordination, was supported by semiempirical MNDO [11] and PM3 [12, 13] frequency calculations. *Ab initio* calculations with the basis sets STO-3G and 3-21G were performed to verify the semiempirical results with regard to structural features.

Experimental

Spectroscopic investigations

IR spectra were recorded on benzene solutions and KBr pellets using a Bruker model IFS 25 spectrometer with a resolution of 4 cm^{-1}. Raman spectra of benzene solutions were excited with the 514 nm line of an argon ion laser (Spectra Physics model 166), the 647 and 676 nm lines of a krypton ion laser (Spectra Physics model 2020) and the 1064 nm line of a Nd-YAG laser (MBB Medilas 2). For Raman spectra of crystalline samples, a micro Raman setup (514 nm excitation, Spectra Physics model 2016, Dilor XY triple spectrograph) [14] was used. The resolution was 4 cm^{-1}.

UV–Vis absorption spectra were taken on benzene solutions using a Perkin-Elmer model Lambda 19 spectrophotometer.

Reaction of 1,3-dimethylbenzo[b]naphtho[1,2-d]pyran-6-one (1) with $AlCl_3$

A solution of 0.1 g (0.365 mmol) **1** in 50 cm^3 dry benzene was treated with an equimolar amount of 0.05 g (0.375 mmol) $AlCl_3$. The reaction mixture was stirred for 1 h at room temperature under an argon atmosphere. The benzene solution of the resulting complex **4** was used for spectroscopic examinations. ^1H NMR (C_6D_6): $\delta = 1.90$ (s, 3H, 1-CH_3), 2.03 (s, 3H, 3-CH_3), 6.64 (s, 1H, 4-H or 2-H), 6.89 (s, 1H, 2-H or 4-H), 7.06–7.26 (m_c, 2H, 10-H and 11-H), 7.37 (d, $J = 8.28$ Hz, 1H, 8-H or 7-H), 7.45 (d, $J = 8.12$ Hz, 1H, 9-H), 7.65 (d, $J = 8.12$ Hz, 1H, 12-H), 8.22 (d, $J = 8.42$ Hz, 1H, 7-H or 8-H).

Calculations

The semiempirical methods PM3 and MNDO were used to determine the geometry and vibrational frequencies of 1,3-dimethylbenzo[*b*]naphtho[1,2-*d*]pyran-6-one (**1**) and its $AlCl_3$ complex **4**. Additionally, the resulting geometric data were compared with those obtained by *ab initio* calculations as well as by X-ray diffraction on **1** [15].

The semiempirical RHF calculations were performed by means of the VAMP 4.5 [16] program package. First the geometry was optimized using the original algorithm by Baker [17]. At the stationary point, a force calculation was carried out in order to determine the frequencies of molecular vibrations. As SCF methods are known to overestimate force constants, several empirical scaling procedures have been suggested [18, 19]. We found linear scaling produced results with satisfying accuracy. Therefore the resulting values were scaled with reference to the experimental $\nu(C{=}O)_{exo}$ mode. For the PM3 frequencies, we ascertained a linear scaling factor of 0.864, while the MNDO scaling factor was set to 0.818 to get better agreement with experimental results. In order to characterize calculated vibrations, atom pairs, significantly contributing to the energy of a normal mode, are listed with the corresponding energy participation. The *ab initio* RHF calculations were performed using the Gaussian 92 [20] program. The low level basis set STO-3G and the higher level 3-21G basis set were used to obtain structural data. These calculations were performed choosing the direct SCF option. Unfortunately, it was not possible to calculate fre-

quencies on the *ab initio* level within reasonable CPU times.

While the different methods did not yield exactly the same values with regard to structural data, all qualitative effects on coordination were nicely reproduced by each calculation performed. Experimental vibrational modes could be assigned by means of semiempirical frequency calculations with a satisfying degree of reliability.

Results and discussion

Structural properties of complex 4

Our calculation results describe the conformation of the six-membered lactone ring of **1** as a twist-boat, which is in agreement with the X-ray data [15]. The dihedral angle C4–C1–C2–C3 (Fig. 1), characterizing the torsion at the biaryl axis is calculated to be between 32.9° (*ab initio*, 3-21G) and 37.6° (MNDO) (Table 1). The $AlCl_3$ complex also has a twist-boat conformation with regard to the lactone part of the molecule. Our calculations predict the Al fragment to be coordinated *cis* to the endocyclic oxygen O21 as shown in Fig. 1*. We suppose an additional electrostatic interaction between the aluminum atom and the endocyclic oxygen to be responsible for this orientation, besides possible unfavorable steric interaction between H28 and one of the chlorine substituents. The bond distances between the carbonyl carbon C7 and the exocyclic oxygen O21 are significantly increased compared to those of the free lactone, whereas the opposite effect is observed for the bond between the carbonyl carbon C7 and the endocyclic oxygen O8. In addition, we find smaller values for the torsion angles C6–O8–C7–C5 and C4–C1–C2–C3 for the complex while the dihedral angles C1–C2–C3–C12 and (with the exception of the PM3 results) C20–C4–C1–C2 slightly increase. The sum of values corresponding to the latter three dihedral angles, the 'inner spiral loop' of the molecule [15], remains practically unchanged on complexation, while the heterocyclic lactone ring is significantly planarized.

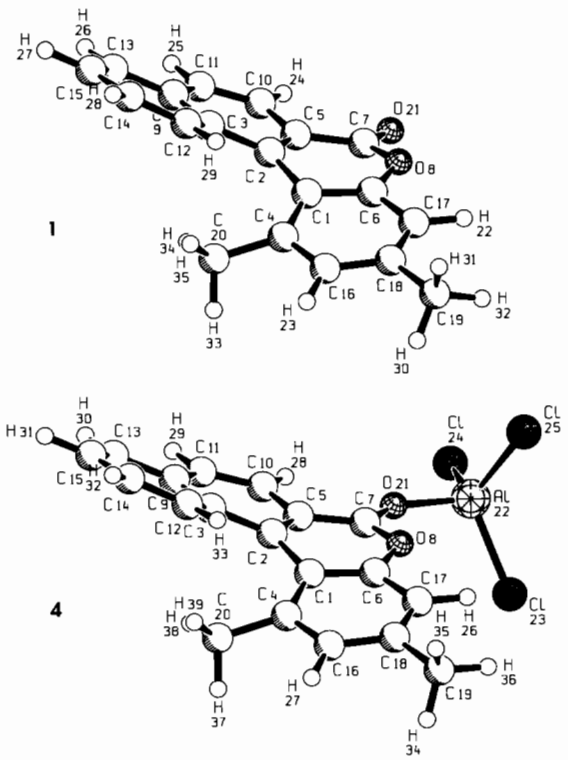

Fig. 1. Structures of lactone **1** and its $AlCl_3$ complex **4** as obtained by *ab initio* (3-21G) calculations.

*Besides structure **4**, other, e.g. two-fold, complexed species cannot completely be excluded at this point.

The structural parameters that differ most distinctly on coordination of $AlCl_3$ to lactone **1**, are listed in Table 2.

All these effects lead to the conclusion that the resonance structure **4b** (Scheme 3) contributes significantly to a description of the geometry of the complex. The planarization of the central lactone ring can be explained in terms of two cooperating effects that are both based on an increased sp^2-character of the endocyclic oxygen O8 in the complex compound: the lowered degree of hybridization on O8 leads to a direct reduction of the dihedral angle C6–O8–C7–O5. Additionally, the contraction of the C7–O8 bond reduces the sterical repulsion between the methyl group C20 *ortho* to the biaryl axis and the naphthyl part. A further planarizing force should be the complexation induced partial positive charge to be delocalized.

UV–Vis properties of the complex

All these calculated changes in geometry, as resulting from the coordination and the mentioned partial charge, increase the conjugation between the π-systems of the naphthyl and the phenyl part of the molecule. UV–Vis absorption measurements show the electronic absorption edge to be shifted from 390 nm of the free lactone to 480 nm of the complex, while no further changes can be detected up to 1300 nm. The result of higher conjugation can also be observed as a change from colorless for the free lactone **1** to a bright fluorescent yellow for the $AlCl_3$ complex **4**.

Vibrational characteristics

The IR and Raman spectra of the free pyranone **1** in solution and solid state are listed in Table 3. The vibrational assignment is based upon previously reported results from a normal coordinate analysis on the unsubstituted lactone compound (H instead of Me) [10]

TABLE 1. Selected distances (Å) and dihedral angles (°) of lactone **1** and its $AlCl_3$ complex **4**. α:C20–C4–C1–C2; β: C4–C1–C2–C3; γ: C1–C2–C3–C12; $\Sigma_{\alpha\beta\gamma}$ = total sum of dihedral angles α, β and γ; δ: C6–O8–C7–C5

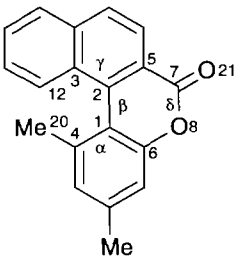

System	Calculation method	Distance C7–O21	Distance O8–C7	Angle α	Angle β	Angle γ	$\Sigma_{\alpha\beta\gamma}$	Angle δ
1	MNDO	1.224	1.382	16.5	37.6	19.0	73.1	29.5
	PM3	1.212	1.387	14.6	33.9	16.1	64.6	22.0
	ab initio (STO-3G)	1.217	1.409	10.2	36.0	14.5	60.7	38.9
	ab initio (3-21G)	1.199	1.371	13.4	32.9	16.5	62.8	22.8
	X-ray[a]	1.203	1.363	12.4	34.1	15.0	61.5	24.7
4	MNDO	1.255	1.352	16.7	35.6	20.9	73.2	20.6
	PM3	1.255	1.347	13.3	32.5	18.2	64.0	17.0
	ab initio (STO-3G)	1.266	1.349	11.7	31.8	16.9	60.4	21.2
	ab initio (3-21G)	1.250	1.316	14.1	30.6	17.8	62.5	14.6

[a]See ref. 15.

TABLE 2. Differences in distances (Å) and dihedral angles (°) caused by coordination of **1** to $AlCl_3$

Calculation method	Distance C7–O21	Distance O8–C7	Angle α	Angle β	Angle γ	$\Sigma_{\alpha\beta\gamma}$	Angle δ
MNDO	0.031	−0.030	0.2	−2.0	1.9	0.1	−8.9
PM3	0.043	−0.040	−1.3	−1.4	2.1	−0.6	−5.0
Ab initio (STO-3G)	0.049	−0.060	1.5	−4.2	2.4	−0.3	−17.7
Ab initio (3-21G)	0.051	−0.055	0.7	−2.3	1.3	−0.3	−8.2

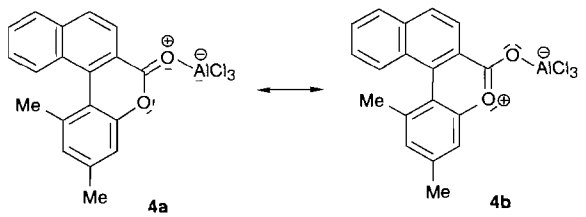

Scheme 3. Resonance structures of the complex **4**.

as well as on data from the presently performed semi-empirical calculations. For the complex compound the most characteristic IR absorption bands are given in Table 4, together with the corresponding bands of the free pyranone and an approximate vibrational description. The experimentally observed values are compared with the calculated ones, for both the pyranone and the complex. For the sake of clarity only those bands are listed that show significant shifts on coordination. Unfortunately, Raman spectra excited at 514, 647, 676 and even 1064 nm were superimposed by an extraordinarily strong fluorescence, thus no appreciable conclusion could be drawn from these experiments.

As reported earlier on simpler systems [21–23], coordination shifts in the vibrational spectra of Lewis acid carbonyl complexes can be interpreted in terms of the valence changes resulting from complexation, as shown in Scheme 2. Particularly, a decrease in frequency for the exocyclic ν(C=O) vibration (due to diminished bond order) is expected. Vibrations including the endocyclic C–O stretching coordinate should be shifted to higher frequencies due to the increased bond order in this case. The majority of vibrations, especially of the aryl systems, should be much less affected. Our calculations indeed delivered the expected coordination shifts (Table 4).

The strongest effect is observed for the exocyclic ν(C=O) mode that shifted from 1728 to 1576 cm^{-1} on coordination ($\Delta\nu_{obs} = -152$ cm^{-1}; $\Delta\nu_{scaled}$(PM3) = -135 cm^{-1}; the MNDO value ($\Delta\nu_{scaled} = -110$ cm^{-1})

TABLE 3. Vibrational spectrum of **1**[a]

Wavenumbers (cm^{-1})				Mode number	Approximate description
IR(C_6H_6)	IR(KBr)	Ra(C_6H_6)	Ra(Cryst.)		
1728vs	1720vs	1732m	1708s	ν_{11}	$\nu(C{=}O)_{exo}$
1616s	1615s	1612m	1609m	ν_{12}	$\nu(C{=}C)_{arom}$
1596w	1602sh	1602m	1590vw	ν_{13}	$\nu(C{=}C)_{arom}$
1576sh	1573sh	1571sh*	1565w	ν_{14}	$\nu(C{=}C)_{arom}$
n.o.*	1558w	1552w	1548vw	ν_{15}	$\nu(C{=}C)_{arom}$
		1504m	1505w	ν_{16}	$\nu(C{=}C)_{arom}$
		1478w	1483vw	ν_{17}	$\nu(C{=}C)_{arom}$
n.o.*	1462w	1455w	1457m	ν_{18}	$\delta(arom)_{ip} + \nu(C{=}C)_{arom}$
1444sh*	1442m			ν_{19}	$\delta(arom)_{ip} + \nu(C{=}C)_{arom}$
		1429w	1428w	ν_{20}	$\delta(arom)_{ip} + \delta(arom)_{oop}$
n.o.*	1390w	1384s	1383s	ν_{21}	$\delta(arom)_{ip} + \nu(C{=}C)_{arom}$
1372w	1370m	1366s	1364vs	ν_{22}	$\delta(arom)_{ip} + \nu(C{=}C)_{arom}$
1342w	1344m			ν_{24}	$\nu(C{=}C)_{arom} + \delta(arom)_{ip}$
1304m	1301s	1297vw	1296vw	ν_{25}	$\nu(C{=}C)_{arom} + \delta(arom)_{ip}$
			1270vw	ν_{27}	$\nu(C{=}C)_{arom} + \delta(arom)_{ip}$
1252m	1257m	1249m	1250m	ν_{28}	$\nu(C{=}C)_{arom} + \delta(arom)_{ip}$
1228w	1230m	1226sh	1228w	ν_{29}	$\delta(arom)_{ip}$
1202sh*	1204w	1210vw	1209w	ν_{30}	$\nu(C{=}C)_{arom} + \delta(arom)_{ip}$
		1198vw	1197w	ν_{31}	$\nu(C{=}C)_{arom} + \delta(arom)_{ip}$
n.o.*	1158s	1141vw	1142vw	ν_{32}	$\delta(arom)_{ip}$
1108m	1107vs			ν_{35}	$\nu(C{=}C)_{arom} + \nu(C{-}O)_{endo}$
1088m	1090m	1084w	1087vw	ν_{36}	$\nu(C{=}C)_{arom} + \nu(C{-}O)_{endo}$
1050m	1036s	1057vw	1055vw	ν_{37}	$\delta(arom)_{oop}$
n.o.*	1041w			ν_{38}	$\nu(C{=}C)_{arom} + \delta(arom)_{oop}$
		1022sh*	1026vw	ν_{39}	$\nu(C{=}C)_{arom} + \delta(arom)_{ip}$
992sh*	985w			ν_{42}	$\nu(C{=}C)_{arom} + \delta(arom)_{oop}$
968sh*	964w			ν_{44}	$\nu(C{=}C)_{arom}$
890sh*	889w			ν_{47}	$\delta(arom)_{oop}$
n.o.*	858m			ν_{49}	$\delta(arom)_{oop}$
n.o.*	825m	824sh*	822w	ν_{50}	$\delta(arom)_{ip} + \delta(arom)_{oop}$
802w	800m			ν_{51}	$\delta(arom)_{ip} + \delta(lac)_{oop}$
764s	756vs			ν_{53}	$\delta(arom)_{oop} + \delta(lac)_{oop}$
730m	729m			ν_{54}	$\delta(arom)_{ip} + \delta(arom)_{oop}$
		686w	686m	ν_{57}	$\delta(arom)_{oop}$
n.o.*	662w	667vw	666vw	ν_{58}	$\delta(arom)_{oop}$

[a]Mode numbering and description according to ref. 10; n.o.: not observed; *: obscured by solvent bands; arom: aromatic ring system; lac: lactone bridge; ip: in plane; oop: out of plane; *exo*: exocyclic; *endo*: endocyclic; vs: very strong; s: strong; m: medium; w: weak; vw: very weak.

is calculated too small). A reason for this high value, compared with those reported earlier for simple carboxylic ester $AlCl_3$ complexes ($\Delta\nu = -80$ to $-120\ cm^{-1}$) [22, 24–26], may be seen in the extended planarized aromatic system, which serves as efficient +M substituent. Using a highly simplified force-field treatment of an $AlCl_3X$ framework, Jones and Wood [27] found that there is a good correlation between the decrease in the $\nu(C{=}O)$ frequency and the Al–X force constant (which might have values from 0.5 and 2.0 mdyn $Å^{-1}$). The application of their model results in an approximate Al–O force constant of 1.3 mdyn $Å^{-1}$ (130 Nm^{-1}) for the present complex.

In the mid-frequency range we observed the disappearance of two lactone bands (1088 and 1108 cm^{-1}) after complexation. The assumption that these bands could be shifted to higher frequencies and therefore might be overlapped by the strong and broad solvent signal at 1176 cm^{-1} in the complex spectrum, could be confirmed by the means of difference spectra. Thus, we could locate the corresponding bands at 1124 and 1160 cm^{-1}, respectively ($\Delta\nu_{obs} = +36\ cm^{-1}/+52\ cm^{-1}$; $\Delta\nu_{scaled}(PM3) = +20\ cm^{-1}/+22\ cm^{-1}$). The MNDO calculation also qualitatively describes these shifts, however the values corresponding to this method are too small ($\Delta\nu_{scaled}(MNDO) = +10\ cm^{-1}/+8\ cm^{-1}$). Furthermore, the 1228 cm^{-1} band is found to be shifted to 1268 cm^{-1} ($\Delta\nu_{obs} = +40\ cm^{-1}$; $\Delta\nu_{scaled}(PM3) = +54\ cm^{-1}$; $\Delta\nu_{scaled}(MNDO) = +76\ cm^{-1}$). This behavior suggests that all those vibrations involve significant endocyclic C–O stretching. Our calculations confirm this at least for the two higher frequency bands (Table 4)

TABLE 4. Experimental and calculated (scaled) vibrational frequencies, energy contributions, and coordination shifts $\Delta\nu$ of **1** and its $AlCl_3$ complex **4** in benzene[a]

System	ν[IR(C_6H_6)] (cm^{-1})	Calculated (cm^{-1})		Contribution (%)				Approximate description	$\Delta\nu$ (cm^{-1})		
		PM3	MNDO	PM3		MNDO			exp.	PM3	MNDO
1	1728	1728	1728	C7–O21	48.0	C7–O21	53.5	ν(C=O)$_{exo}$			
				C5–C7	22.4	C5–C7	23.4	+ ν(C–C)$_{endo}$			
				C7–O8	21.0	C7–O8	22.5	+ ν(C–O)$_{endo}$			
				O8–O21	7.4	C5–C10	0.1				
	1228	1167	1203	C7–O8	11.1	C7–O8	16.5	ν(C–O)$_{endo}$			
				C6–C17	6.9	C5–C7	9.3	+ ν(C–C)$_{endo}$			
				C5–C7	6.5	C7–O21	7.6	+ ν(C=O)$_{exo}$			
				C7–O21	6.0	C13–H26	4.8				
	1108	1139	1143	C4–C16	9.7	C7–O8	10.1	ν(C–O)$_{endo}$			
				C1–C4	8.8	C10–C11	7.8	+ ν(C=C)$_{arom}$			
				C7–O8	7.2	C9–C11	7.0				
				C16–C18	6.2	C2–C5	6.6				
	1088	1085	996	C2–C3	9.9	C9–C11	8.0	ν(C=C)$_{arom}$			
				C3–C9	9.6	C2–C3	7.9				
				C9–C13	8.1	C9–C13	7.9				
				C3–C12	8.0	C3–C12	6.9				
4	1576	1593	1618	C7–O21	29.2	C7–O21	47.9	ν(C=O–Al)$_{exo}$	−152	−135	−110
				C5–C7	17.7	C5–C7	22.0	+ ν(C–C)$_{endo}$			
				C7–O8	16.3	C7–O8	21.4	+ ν(C–O)$_{endo}$			
				C7–Al22	15.9	O21–Al22	7.9				
	1268	1221	1279	C7–O8	13.1	C7–O8	19.4	ν(C–O)$_{endo}$	+40	+54	+76
				C7–O21	6.0	C5–C7	14.4	+ ν(C=O–Al)$_{exo}$			
				C7–Al22	5.9	C7–O21	10.3	+ ν(C–C)$_{endo}$			
				C5–C7	5.8	C6–C17	4.7				
	1160sh*	1161	1151	C6–C7	12.8	C2–C5	9.1	ν(C=C)$_{arom}$	+52	+22	+8
				C16–C18	9.0	C10–C11	8.5				
				C1–C4	8.6	C9–C11	8.1				
				C17–C18	8.2	C13–C15	6.1				
	1124sh*	1105	1006	C2–C3	11.2	C14–H32	9.1	ν(C=C)$_{arom}$	+36	+20	+10
				C3–C9	8.9	C9–C13	8.5				
				C9–C13	8.0	C2–C3	8.2				
				C3–C12	7.4	C9–C11	7.9				
	538	613	464	C5–C7	8.3	Al22–Cl24	24.8	ν($AlCl_3$)$_E$			
				C6–O8	6.4	Al22–Cl25	22.7	+ ν(Al–O)			
				O8–O21	6.4	O21–Al22	15.6				
				O8–Al22	6.1	Al22–Cl23	15.5				
	436	440	462	C5–C7	6.1	Al22–Cl23	29.4	ν($AlCl_3$)$_{A_1}$			
				O8–O21	6.1	Al22–Cl25	21.7	+ ν(Al–O)			
				O21–Al22	5.5	Al22–Cl24	18.8				
				C7–O8	4.5	O21–Al22	17.4				

[a]Only modes that are observed to be shifted or additionally appear on coordination are mentioned. *: obscured by solvent peaks, revealed from difference spectra; sh: shoulder.

whereas the 1088 cm^{-1} band (of **1**) should involve mainly aromatic C=C stretching. The observed shift of this frequency ($\Delta\nu_{obs} = +36$ cm^{-1}) indicates an influence on the π-skeleton of the molecule, supported by the strong red shift of the UV-absorption edge. The residual lactone bands remain essentially unchanged on complexing, which is in good agreement with the calculated frequency data.

Below 700 cm^{-1}, a couple of new bands arising from vibrations of the generated $OAlCl_3$ framework are expected. We observed a very strong IR band at 538 cm^{-1} that can be assigned to degenerate O–$AlCl_3$ stretching ν_4. A weak feature about 100 cm^{-1} lower can be attributed to the corresponding symmetric ν_2 mode. As our MNDO results show, these modes are best described as Al–Cl stretching vibration with con-

siderable Al–O stretching contribution. This assignment agrees with that established earlier by Jones and Wood, who observed very similar frequencies for ν_2 and ν_4 in ether and ester complexes of $AlCl_3$ and thoroughly discussed the nature of these vibrations [23, 25–27].

Conclusions

As can be seen, the calculated changes in geometry as well as in the vibrational behavior of lactone on coordination to $AlCl_3$, agree well with the experimental data. The combination of frequency calculations and vibrational spectroscopy has proved to be a suitable method for understanding the relationship between changes in conformation and vibrational behavior.

In the special case of the sensitive $AlCl_3$ lactone complex **4**, for which X-ray data are not available, the quantum chemical calculations are an important tool for gaining information about even small effects on coordination. Besides changes in binding characters $(C–O)_{exo}$ and $(C–O)_{endo}$, which could also be observed by means of vibrational spectroscopy, an increased planarization of the central lactone part of the complexed molecule is predicted by our calculations. In earlier investigations on transition metal complexes of similar biaryl lactones [8], we could observe such a planarization by X-ray diffraction.

This work represents an important step towards the knowledge of Lewis acid catalyzed atropisomer-selective ring opening reactions. Investigations on the influence of Lewis acids on the helimerization barrier are in progress [28].

Acknowledgements

We gratefully acknowledge financial support from the Deutsche Forschungsgemeinschaft (Sonderforschungsbereich No. 347 'Selektive Reaktionen Metallaktivierter Moleküle', Projects B-1 and C-2) as well as from the Fonds der Chemischen Industrie. We also thank E. Dombrowski and K.-P. Gulden for their valuable technical assistance.

References

1 G. Bringmann, B. Schöner, K. Peters, E.-M. Peters and H.G. von Schnering, *Liebigs Ann. Chem.,* (1994) 439.
2 G. Bringmann, R. Walter and R. Weirich, *Angew. Chem., 102* (1990) 1006; *Angew. Chem., Int. Ed. Engl., 29* (1990) 977.
3 G. Bringmann and T. Hartung, *Tetrahedron, 49* (1993) 7891.
4 G. Bringmann, R. Walter and Ch.L.J. Ewers, *Synlett,* (1991) 581.
5 G. Bringmann, Ch.L.J. Ewers, L. Göbel, T. Hartung, B. Schöner and R. Walter, in H. Werner, A.G. Griesbeck, W. Adam, G. Bringmann and W. Kiefer (eds.), *Selective Reactions of Metal-Activated Molecules,* Vieweg, Braunschweig, Germany, 1992, p. 183.
6 G. Bringmann, L. Göbel and O. Schupp, *GIT Fachz. Lab., 3* (1993) 189.
7 T. Ertel, S. Hückmann, H. Bertagnolli, G. Bringmann, Ch. Ewers, G. Erker, I. Hart and Ch. Sarter, in S.S. Hasnain (ed.), *X-Ray Absorption Fine Structure*, Ellis Horwood, New York, 1991, p. 562.
8 G. Bringmann, O. Schupp, K. Peters, L. Walz and H.G. v. Schnering, *J. Organomet. Chem., 438* (1992) 117.
9 T.A. Mohamed, H.D. Stidham, G.A. Guirgis, H.V. Phan and J.R. Durig, *J. Raman Spectrosc., 24* (1993) 1.
10 T. Grimm, A. Ellebracht, W. Kiefer, G. Bringmann and H. Busse, *Vib. Spectrosc., 5* (1993) 181.
11 M.J.S. Dewar and W. Thiel, *J. Am. Chem. Soc., 99* (1977) 4899.
12 J.J.P. Stewart, *J. Comput. Chem., 10* (1989) 209.
13 J.J.P. Stewart, *J. Comput. Chem., 10* (1989) 221.
14 M. Lankers, D. Göttges, A. Materny, K. Schaschek and W. Kiefer, *Appl. Spectrosc., 46* (1992) 1331.
15 G. Bringmann, T. Hartung, L. Göbel, O. Schupp, Ch.L.J. Ewers, B. Schöner, R. Zagst, K. Peters, H.G. v. Schnering and Ch. Burschka, *Liebigs Ann. Chem.,* (1992) 225.
16 G. Rauhut, J. Chandrasekhar and T. Clark, *VAMP 4.5,* Universität Erlangen-Nürnberg, Germany, 1992.
17 J. Baker, *J. Comput. Chem., 8* (1987) 563.
18 P. Pulay, G. Fogarasi, F. Pang and J.E. Boggs, *J. Am. Chem. Soc., 101* (1979) 2550.
19 P. Pulay, G. Fogarasi, X. Zhou and P.W. Taylor, *Vib. Spectrosc., 1* (1990) 159.
20 M.J. Frisch, G.W. Trucks, M. Head-Gordon, P.M.W. Gill, M.W. Wong, J.B. Foresman, B.G. Johnson, H.B. Schlegel, M.A. Robb, E.S. Replogle, R. Gomberts, J.L. Andres, K. Raghavachari, J.S. Binkley, C. Gonzalez, R.L. Martin, D.J. Fox, D.J. Defrees, J. Baker, J.J.P. Stewart and J.A. Pople, *Gaussian 92,* Revision C, Gaussian Inc., Pittsburgh, PA 1992
21 M.F. Lappert, *J. Chem. Soc.,* (1961) 817.
22 M.F. Lappert, *J. Chem. Soc.,* (1962) 542.
23 D.E.H. Jones and J.L. Wood, *J. Chem. Soc.,* (1971) 3132.
24 M.F. Lappert and J.K. Smith, *J. Chem. Soc.,* (1965) 5826.
25 D.E.H. Jones and J.L. Wood, *J. Chem. Soc.,* (1967) 1140.
26 D.E.H. Jones and J.L. Wood, *J. Chem. Soc.,* (1971) 3135.
27 D.E.H. Jones and J.L. Wood, *J. Chem. Soc.,* (1966) 1448.
28 G. Bringmann and U. Dauer, in preparation.